Colloid Polym Sci 273:544–558 (1995)

ORIGINAL CONTRIBUTION

M.M. Jacobi
V. Abetz
R. Stadler
L. de Lucca Freitas
W. Gronski

Polybutadiene model networks – synthesis, mechanical characterization and comparison with rubber elasticity models

Received: 3 February 1992
Accepted: 7 February 1995

M.M. Jacobi · L. de Lucca Freitas
Instituto de Quimica
Universidade Federal de Rio Grande do Sul
Avenida Bento Gonclaves 9500
91501-970 Porto Alegre, Brazil

V. Abetz · Dr. R. Stadler (✉)
Institut für Organische Chemie
Johannes-Gutenberg-Universität
J.J. Becher Weg 18-20
55099 Mainz, FRG

W. Gronski
Institut für Makromolekulare Chemie
Albert-Ludwigs-Universität
Stefan-Meier-Straße 31
79104 Freiburg, FRG

Abstract Model networks of defined crosslink density are prepared via nonradical statistical crosslinking of polybutadiene in bulk and concentrated solution using a masked bistriazolinedione as crosslinker. The kinetics of crosslinking is monitored by FT-IR-spectroscopy. The reaction follows pseudo-1st-order reaction kinetics. The activation parameter of the crosslinking reaction is estimated from crosslinking at various temperatures. Networks of deuterated polybutadiene are prepared by this reaction in a wide range of crosslink densities. The stress strain behavior is analyzed according to the Junction Constraint-Theory of rubber elasticity (JCT) and to the approach introduced by Graessley accounting for trapped topological constraints. The analysis clearly demonstrates that trapped entanglements contribute to the mechanically effective cycle rank, i.e., to the modulus in this system in the small and large strain limit.

Key words Polybutadiene – random crosslinking – rubber elasticity – trapped entanglements

Introduction

The understanding of rubbery materials is strongly dependent on the availability of suitable model networks [1–3]. Most often, endlinked networks, i.e., network prepared by reactions of endfunctionalized chains with multifunctional crosslinkers are believed to represent the most close approach to theoretical ideality. However, from a chemists point of view, these model networks are far from being perfect. If the crosslink reaction is not going to complete conversion, ill-defined networks are obtained, characterized by a considerable sol fraction and dangling ends. Statistical crosslinking of long primary chain molecules by a defined chemical reaction might be an alternative to imperfect endlinking chemistry. In addition, such an approach allows studies on networks based on the most important elastomers. Also, a small amount of side reactions ($< 5\%$) will not be as crucial as in the end linking case and changes the total crosslink density only to a small extent. Of course, such a crosslink reaction will result in a length distribution of network strands. If necessary, this can be treated by common laws of statistics. Thus, in the present context, a model network is defined as a system with a controlled number of permanent crosslink junctions, given by the stoichiometry of the reaction and a minimum number of defects like loops and dangling chains. In order to prepare model networks by statistical crosslinking a well-defined crosslink reaction has to be used. Peroxide or sulfur curing as well as radiation chemistry are not really appropriate for this purpose.

Bis-1,2,4-triazoline-3,5-diones **1** have been reported to be efficient crosslinkers for polydienes [4–6]. Crosslinking occurs by a defined ene-reaction [7] without detectable

side reactions. Thus, the first requirement for the synthesis of model networks, introduction of a defined number of chemical linkages, is fulfilled. The main disadvantage is the extremely high reaction rate [6, 8]. As a consequence, homogeneous networks only can be obtained if the reaction is performed in semidilute solutions (3–6 wt%, depending on the solution viscosity). Due to the solution crosslinking process, the major fraction of the crosslinker forms small or medium sized loops, and thus reduces the number of elastically effective chains [6, 9, 10]. From the study of the segmental orientation behavior by ^{2}H-NMR, it has been deduced that the elastic behavior of dry elastomer samples prepared by the solution crosslinking process reflects the unusual network topology of these materials [11]. Analysis of the mechanical behavior of these films cannot be performed by the theory developed by Flory and Erman [12–14] for both polybutadiene and polyisobutylene networks [15]. In terms of the Mooney–Rivlin approach the $2C_2$ parameter (see below) of these solution crosslinked networks is too large ($2C_2 > 2C_1$) to allow a description by the theory.

Based on the work of Green and coworkers [16], we were able to establish a protecting group for the highly reactive bistriazolinedione which allows crosslinking in bulk in a defined manner [17]. In the present paper we report on the detailed kinetics of the crosslinking reaction and describe the analysis of the mechanical properties of a series of polybutadiene networks with widely varying crosslink density ($2000 < M_c < 60000$ g/mol) using the junction constraint theory of rubber elasticity. From the analysis of the mechanical properties of swollen networks information about the confidence range of the network parameters extracted from the theory is obtained. In addition, networks were prepared at various polymer concentrations and constant chemical crosslink density. The parameters obtained from the JCT are compared to the analysis in the small strain limit, originally performed by Dossin and Graessley [2].

Experimental

Materials

Crosslinker

Adamantylidene-adamantane **3**, synthesized as described before [18], was reacted at room temperature stoichiometrically or in slight excess with bis-4,4′-diphenylmethylene-1,2,4-triazolinedione **1** to the bis-diazetidine addition product **4**. The structure of **4** was proven by spectroscopic techniques and elemental analysis. Structural characterization and experimental details are given in ref. [17].

Polybutadiene

1,4-deuterated polybutadiene was obtained by standard anionic high vacuum polymerization techniques using *s*-butyllithium as initiator in cyclohexane as solvent. Details of monomer preparation and purification are given elsewhere [5, 19]. The linear polymers were characterized by GPC and osmometry. 2,6-di-*t*-butyl-4-phenol was added as antioxidant.

In an analogous manner deuterated and undeuterated polybutadiene oligomers ($P_n \sim 20$) were prepared [19, 20]. These will be used as a structurally identical swelling agent for the polybutadiene networks. Sample characterization is summarized in Table 1.

For the kinetic measurements a reprecipitated technical grade cis-1,4-polybutadiene (CB-10, cis-1,4-PB, kindly supplied by CW-Hüls, Marl) was used.

Preparation of the networks

Crosslinking in bulk: The slightly yellow crystals of **4** readily dissolve in unpolar solvents like benzene. Two g of polybutadiene were dissolved in 30–40 ml of benzene and the appropriate amount of **4** dissolved in few ml's of benzene was added. The solutions were degassed (two times) and the solvent was slowly evaporated in a flat-bottomed Petri-dish. No crystallization of the blocked triazolinedione was observed for small amounts of **4**. Uncured PB sheets also can be obtained by freeze drying and subsequent molding of the homogeneous solutions. Film thickness was about 300 μm for the materials used in this study. The uncrosslinked sheets were put into a vacuum

Table 1 Characterization of high- and low molecular weight polybutadients

	M_n (g/mol)	M_w/M_n [b]
Polymers		
CB-10 cis-PB Technical grade	200000[a]	2
PB_d-2[d]	80000[a]	1.34
PB_d-3[d]	370000[a]	1.41
Oligomers		
E-1000[d]	990[c]	1.17
F-1000[e]	750[c]	1.14

[a]) membrane osmometry
[b]) size exclusion chromatography
[c]) vapor pressure osmometry
[d]) degree of deuteration at C_1 and C_4: 65–70 mol%
[e]) non deuterated PBB oligomer
microstructure: 7% 1,2-units, 93%, 1,4-units about equally distributed to cis and trans

oven, heated to 120 °C, where they were kept for 1 h. As will be discussed below, this reaction time is sufficient for complete reaction. In the vacuum oven free **3** is subliming out of the polymer film. Final traces of **3** are removed by swelling in petroleum ether. The samples are dried before subsequent use, and stored in a refrigerator. Two series of networks will be discussed below. In series PB_d-A-xx the lower molecular weight polybutadiene ($M_n = 80\,000$ g/mol) has been used as starting material and the amount of crosslinker was varied between 0.1 and 1.5 mol.-% with respect to the double bonds. In series PB_d-B-xx high molecular weight polybutadiene ($M_n = 370\,000$ g/mol) was used. In that case, three different cross-link densities were prepared. Designation of the samples as well as the results of swelling experiments is given in Table 2. In networks PB_d-A-015 and PB_d-A-010 swelling was so strong that swollen samples could not be weighed to determine the equilibrium degree of swelling, given in Table 2 as the volume fraction of polymer in the swollen gel v_2. No attempts were made to perform a quantitative sol-gel analysis. For network series B and the higher crosslink densities of series A, no notable sol fraction could be obtained from the benzene solution used for the swelling experiments. However, a rather large, though not quantified sol fraction was detected in the lowest crosslink densities of the A-series.

The swelling behavior of network series A and B is quite different. At the same crosslink densities smaller swelling is observed for series B. As will be discussed below, this cannot be exclusively attributed to a larger number of dangling chains in the networks present in series A.

Table 2 Networks prepared by bulk crosslinking of deuterated polybutadiene; series A and B

Sample	Reacted	PB_d	BPMTD-Ad_2	v_2
	>C=C< (mol-%)	(g)	(4) (g)	
PB_d-A-010	0.1	1.5	0.013	–
PB_d-A-015	0.15	1.5	0.019	–
PB_d-A-020	0.2	1.5	0.025	0.065
PB_d-A-035	0.35	1.5	0.043	0.107
PB_d-A-050	0.5	1.5	0.062	0.140
PB_d-A-075	0.75	1.5	0.093	0.146
PB_d-A-100	1.0	1.5	0.123	0.154
PB_d-A-150	1.5	1.5	0.186	0.206
PB_d-B-025	0.25	3	0.124	0.115
PB_d-B-030	0.3	3	0.149	0.120
PB_d-B-060	0.6	3	0.297	0.216

v_2 = volume fraction of the polymer after equilibrium swelling in benzene at 25 °C

Samples for IR spectroscopy were obtained by casting a thin film (10–20 μm) onto a KBr pellet. In that case the cis-1,4-PB has been used and the amount of crosslinker was kept constant.

In some preliminary experiments pellets of about 1 mm thickness were used as test specimen in a Rheometrics Solid Analyzer (RSA II) in the dynamic compression mode to study crosslinking in the dynamic mechanical experiment. For these measurements a lower molecular weight polybutadiene (PB_n-50, $M_n = 50\,000$ g/mol) has been used.

Preparation of networks in concentrated polymer solution: As has been mentioned above, crosslinking has been performed previously in dilute solution [5, 9, 11]. The masked bistriazolinediones now allow crosslinking in concentrated solutions. To study the influence of polymer concentration during network preparation a series of samples (PB_d-L-xx) at constant chemical crosslink density was prepared, by varying the volume fraction at the curing reaction v_{2c}. The polymer volume fraction at crosslinking v_{2c} was varied between 1 and 0.08, crosslinker concentration was kept at 0.5 mol%. Mesitylene was used as a solvent because it allows preparation at the same conditions as in bulk without evaporation of the solvent during crosslinking. The networks of this series were prepared simultaneously to allow complete comparability. In the sample with $v_{2c} = 0.08$ partial deswelling was observed at the end of the reaction. This observation will be important in the discussion of the mechanical results. Details of sample preparation as well as the results of equilibrium swelling in benzene are given in Table 3.

Preparation of swollen networks

Strips of $30 \cdot 5 \cdot 0.3$ mm^3 were cut from the cured samples (series B only) and put into a Petri dish. The appropriate

Table 3 Reaction conditions for crosslinking in concentrated solution

Sample	v_{2c}	v_2	Weight PB[a] (g)	Mesitylene in mixture[b] (g)
PB_d-L-008	0.08	0.022	1.346	14.386
PB_d-L-015	0.15	0.027	1.263	6.646
PB_d-L-025	0.25	0.046	1.114	3.105
PB_d-L-050	0.50	0.083	1.424	1.323
PB_d-L-075	0.75	0.117	1.479	0.458
PB_d-L-100	1.00	0.212	1.283	–

[a]) polymer density: 0.93 g/ml
[b]) density of mesitylene: 0.864 g/ml
v_{2c} polymer volume fraction during crosslinking
v_2 polymer volume fraction after equilibrium swelling in benzene at 25 °C

amount of deuterated or nondeuterated oligomers is distributed on the surface of the film. After several days, the free oligomer chains are diffused homogeneously into the network. Practically no oligomer can be removed from the surface of the sample. Samples were kept in the refrigerator prior to further use.

Techniques

IR-spectroscopy

IR-spectra were obtained using a Bruker IFS-88 FT-IR-spectrometer at 4 cm^{-1} resolution. Thirty-two scans were accumulated for each spectrum during the curing process. Spectral subtraction was performed using the IFS-88 system software. Temperature was controlled using a Specac-temperature chamber (± 1 K).

Stress strain experiments

Strips of $30 \cdot 5 \cdot 0.3\ mm^3$ were put into the clamps of an Instron 1122 tensile testing machine. Measurements were made at room temperature at various crosshead speeds (1, 5, 10 mm/min). In addition, equilibrium stress strain measurements were performed for some samples. Only for the networks with the lowest crosslink densities (PB_d-A-010 and PB_d-A-015) and the networks prepared in semidilute solution (PB_d-L-008 and PB_d-L-015) were notable differences ($>3\%$) between the stress strain curves at different strain rates observed. Thus, it has to be concluded that the mechanical data obtained at small crosshead speeds are close to equilibrium. The slowest strain rates were used in the following mechanical analysis.

Results and discussion

Synthesis of polybutadiene networks and kinetics of the crosslinking process

Based on work of Greene and coworkers [16] we used adamantylidene-adamantane **3** to block the bistriazolinedione **1**. At room temperature the bisazetidine compound **4** is formed, which, at higher temperatures, undergoes reversible decomposition into the bistriazolinedione **1** and **3** according to the reaction scheme given in Fig. 1. **4** can be mixed in small amounts into polybutadiene. Upon release the crosslinker **1** immediately reacts with the polybutadiene to form the linkage **2**. As has been mentioned in the previous report [17], direct observation of the thermally induced decomposition of **4** and the formation of the

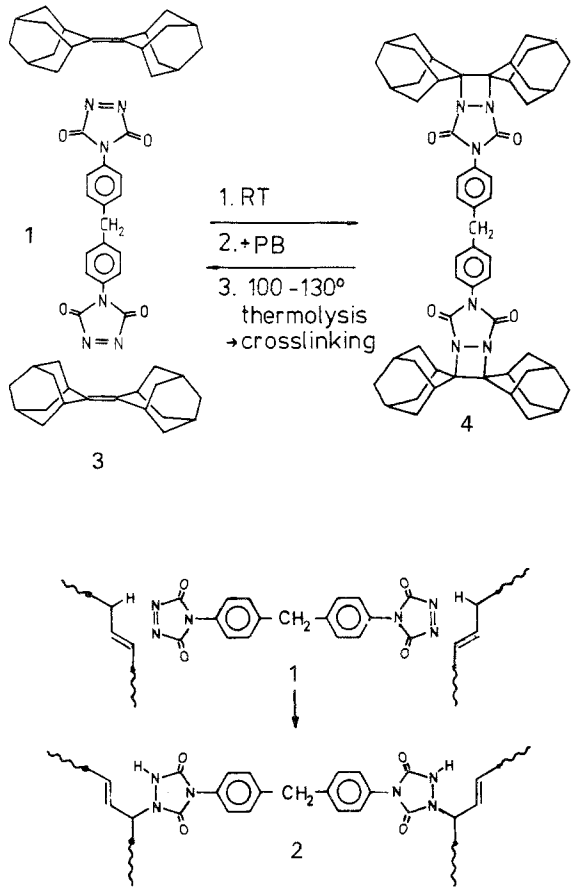

Fig. 1 Reaction scheme for the crosslinking of polybutadiene with a blocked bistriazolinedione; A: blocking and deblocking of the crosslinker; B: crosslink reaction

crosslinks **2** is possible by IR spectroscopy. Because of the high reaction rates of triazolinediones, the reactive enophile **1** cannot be observed in the course of the thermolysis. The vibrations used for the IR-spectroscopic analysis occur between 1300 and 1450 cm^{-1} ($-\mathbf{C}-\mathbf{N}-$ stretching vibrations) and between 1650 and 1850 cm^{-1} ($>\mathbf{C}=\mathbf{O}$ stretching). In the range of 1300 to 1450 cm^{-1} the absorptions due to **4** and **2** are overlapped by absorptions from the polybutadiene, but we have shown that separation of the absorptions is possible using subtraction techniques. In Fig. 2 a typical set of IR-spectra measured at 90 °C is shown in the 1250–1600 cm^{-1} region after subtraction of the polybutadiene. The strong absorption at 1380 cm^{-1} (3 absorption lines) in the spectrum of **4** can be attributed to the –C–N– stretching vibration of the diazetidine system. With increasing curing time the absorptions arising from the four-membered diazetidine ring decrease and the absorption of the unstrained C–N bond in **2** appears in the range of 1400–1440 cm^{-1} with an increasing maximum at 1418 cm^{-1}. The occurrence of the isos-

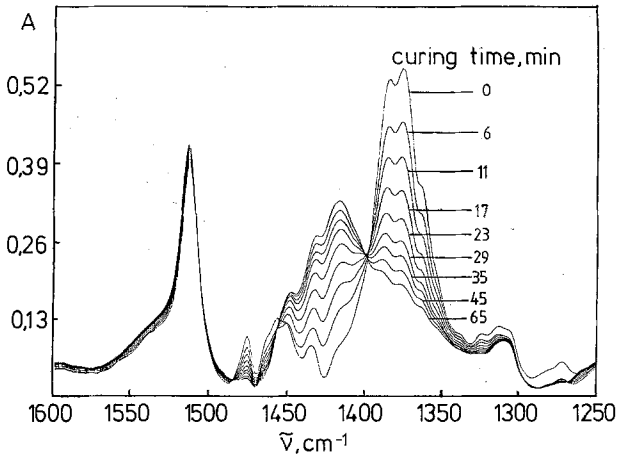

Fig. 2 Curing of polybutadiene with **4** at 90 °C, IR spectra recorded at different curing times; IR-spectrum of the C–N stretching region after subtraction of the polybutadiene

bestic point gives strong evidence that decomposition of **4** and subsequent formation of crosslink **2** occur without notable side reactions of **1**. The same conclusions can be drawn from the analysis of the C=O stretching vibration not shown here [17, 19].

In Fig. 3 the reduced concentration $[\mathbf{4}]/[\mathbf{4}_0]$ obtained from the intensity of the absorption band of at 1378 cm^{-1} is shown as a function of time in a semilogarithmic plot for three different curing temperatures. The concentration of **4** in the polybutadiene was kept constant (1 mol% with respect to the double bonds). Linear plots, corresponding to pseudo-first-order kinetics are obtained for temperatures 80°, 90°, and 100 °C. At higher temperatures the reaction proceeds too rapidly to perform time-resolved FT-IR-spectroscopy using the available equipment. The rate constants are plotted in Fig. 4 as a function of the reciprocal temperature. The activation energy for the thermal decomposition of **4** is about 110 kJ/mol, indicating a very strong temperature dependence of the rate of decomposition. In Table 4, the rate constants and the half times are listed for these temperatures, as well as the rate and half time calculated for 120 °C, where the networks for the mechanical analysis have been prepared. The IR-spectroscopic results show that the reaction proceeds with a high rate at rather low temperatures, where thermal crosslinking of the polybutadiene in the presence of stabilizing agent (2,6-di-t-butyl-4-methyl-phenol) does not occur at comparable reaction times. Though this crosslinking chemistry is limited to the small scale laboratory preparation of elastomer networks, it is of considerable value to synthesize polymer networks with exactly defined number of junctions by statistical crosslinking.

Fig. 3 Kinetic analysis of the polybutadiene curing with **4** at 80°(○), 90°(□) and 100°(△); plot of the reduced concentration $\ln([\mathbf{4}]/[\mathbf{4}_0])$ as a function of the reaction time. $[\mathbf{4}_0]$ = 1 mol-% with respect to the double bonds of polybutadiene

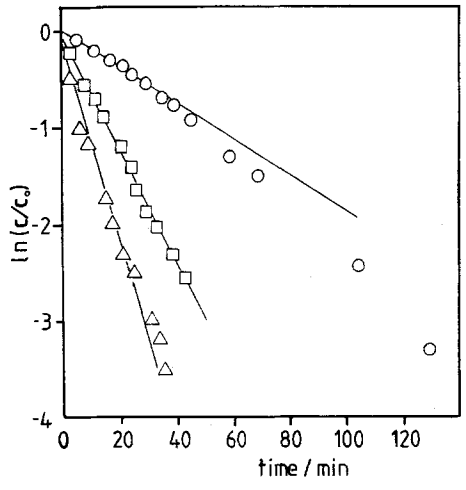

Dynamic-mechanical analysis of the crosslink reaction

As has been shown by Winter and coworkers [21–23], and more recently also by Rubinstein et al. [24], Martin et al.

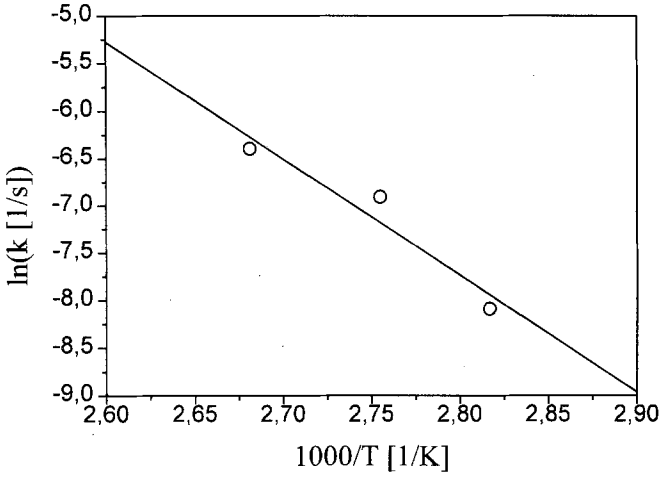

Fig. 4 Arrhenius plot of the reaction rate constant $\ln(k)$ as a function of the reciprocal temperature

Table 4 Rate constants of the thermal decomposition of BPMTD-Ad_2

Temperature (°C)	Rate constant (s^{-1})	Half time (min)
82	$3.07\ 10^{-4}$	37.7
90	$1.00\ 10^{-3}$	11.5
100	$1.67\ 10^{-3}$	7.0
120	$1.1\ 10^{-2}$	1.0

[25], and Macosko et al. [26] dynamic mechanical analysis provides a useful technique to study gelation of networks. Besides a study of Macosko [26] and a work on radiation crosslinking of polyethylene [27], most of the early studies have focused on endlinking chemistry. In Fig. 5 storage and loss modulus as well as loss tangent are plotted for a polybutadiene of molecular weight 50 000 g/mol with 1 mol% crosslinkers at 120 °C as a function of curing time. The values up to 20 min could not be resolved, since the used measurement geometry gives only reliable values for the E^*-modulus above 10^4 Pa. It is evident from this Figure that the reaction is terminated (no further change in the modulus) after about 60 min. Crossover between E' and E'' occurs after about 30 min. The time to complete reaction as deduced from the mechanical data is rather long compared to the half-time obtained from IR spectroscopy. At the beginning of the chemical reaction the probability is high that only one of the two functional groups of the crosslinker has reacted. This means that during the early stages of the reaction only side groups are attached to the polymer backbone, which than further react to give a crosslink. The mechanical spectroscopy detects only the effect of those crosslinker molecules, which have reacted twice. The curing system may be quenched easily due to the high activation enthalpy, thus frequency-dependent measurements below 70 °C could allow a more detailed evaluation of the mechanical properties of highly branched clusters which form during the course of the reaction.

Fig. 5 Dynamic mechanical characterization of the curing process; PB-50000 with 1% crosslinker at 120 °C at 1 rad/s; (measurement performed in a Rheometrics solid analyzer in the parallel plate geometry)

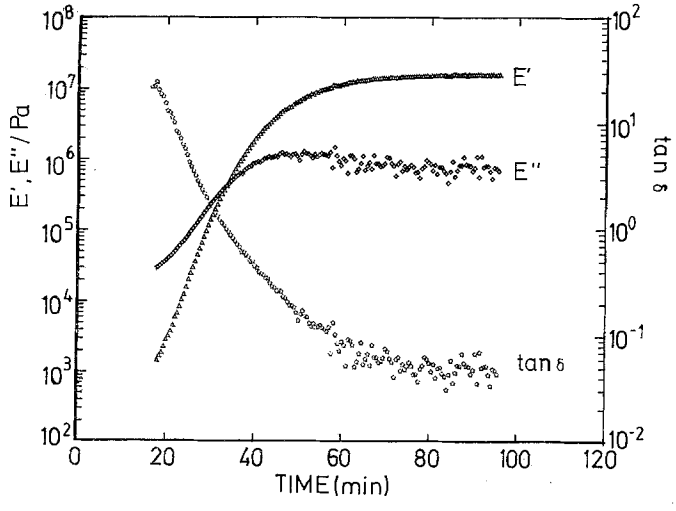

Analysis of the stress-strain behavior using the Flory–Erman junction constraint theory of rubber elasticity and the Graessley–Langley approach

Theoretical background

The stress strain behavior has been analyzed according to different approaches. At small strains the shear modulus $G_{exp} = N_c kT$ was determined and analyzed according to the affine theory [28, 29] which predicts the elastic retractive force of an elastomer as a function of strain λ.

$$f = \frac{NkT}{L_0}(\lambda - \lambda^{-2}); \quad \rho RT/M_c = NkT/L_0 \tag{1}$$

In this equation λ is the deformation with respect to the unperturbed chain dimensions under which the network has been prepared and N/V_0 is the chain density for this situation. In practice, the strain usually is defined with respect to the unstrained length $\alpha = L/L_0$ and the stress strain equation according to the affine theory is given by

$$\sigma = \frac{NkT}{V_f} v_2^{1/3}(V_f/V_0)^{2/3}(\alpha - \alpha^{-2}), \tag{2}$$

where
T: absolute temperature
N: number of elastically effective network chains in the dry sample of volume $V_f (v = N/V_f = \rho/(N_A M_c)$: chain density)
V_0: volume of the sample during crosslinking reaction
N_A: Avogadro's number
ρ: density of the network
v_2: volume fraction of the polymer at measurement.

The reduced force is defined by

$$[f^*] = \frac{\tau \cdot v_2^{-1/3} \cdot v_{2c}^{-2/3}}{(\alpha^2 - \alpha^{-1})} = \frac{\sigma \cdot v_2^{-1/3} \cdot v_{2c}^{-2/3}}{(\alpha - \alpha^{-2})} \tag{3}$$

where
v_{2c}: volume fraction of the polymer at which crosslinking has been performed.
τ: true stress (force per actual cross section)
σ: nominal stress (force per cross-section of the unstrained sample) is predicted to be independent of strain.

An alternative treatment originally developed by James and Guth [30] is the "phantom" theory. In contrast to the affine theory where an affine displacement of the junctions is assumed (sometimes also called junction affine theory), the junctions perform a free Brownian motion around their mean position in the "phantom" theory. It is assumed that the average positions are transformed affinely. The fluctuation around the mean position is strain independent and, as a consequence, the actual deformation of a network chain is nonaffine. Flory [31] has introduced the cycle rank ξ to characterize the network topology of

a Phantom network. ξ is given by the difference between the number of elastically effective chains v and effective junctions μ. For a perfect network of functionality ϕ, the cycle rank ξ is given by

$$\xi = v - \mu = v(1 - 2/\phi) . \tag{4}$$

The strain dependence of the force resulting from the phantom theory is the same as for the affine theory, but the front factors are different by a factor of two for a tetrafunctional network.

$$f_{ph} = \xi kT \cdot v_2^{1/3} \cdot v_{2c}^{2/3} \cdot (\alpha - \alpha^{-2}) \tag{5}$$

The fact that chains cannot cross each other is neglected by the phantom theory. Several attempts have been made to account for this lack in the basic theory, which is equivalent to the search of incorporating the effect of short and long range topological constraints. It is generally accepted that topological interactions have a localized effect on the mobility of junction points. According to Flory and Erman [12–14], this is the only additional contribution necessary to account for the difference between the experimental stress strain data and Phantom theory which is taken as the limiting situation. Experimental results, including those of Graessley [2] and Macosko [26] indicate that the modulus at small strains is not only given by the concentration of elastically effective chains, including the effect of reduced mobility of junction points. Trapped entanglements (long range topological constraints) play an important role in the elastic properties of networks.

The classical theories predict strain independence of the reduced force $[f^*]$. Real networks often are described empirically by the Mooney–Rivlin equation, which gives a linear relation between the reduced force and the reciprocal strain:

$$[f^*] = 2C_1 + 2C_2/\alpha , \tag{6}$$

where $2C_1 = 1/2\rho RT/M_c$ for tetrafunctional networks.

The constants $2C_1$ and $2C_2$ have been determined for many networks, without final conclusive molecular interpretation [2, 29, 32]. $2C_1$ quite often has been identified as the modulus according to the "phantom" theory, while $2C_2$ describes deviations from ideality. Graessley has shown for polybutadiene networks prepared by irradiation crosslinking, that $2C_2$ is dominated by the effect of trapped entanglements [2]. $2C_1$ contained contributions both from the chemical crosslinks and the entanglements.

To interpret the experimental data we will follow the attempts discussed above and determine v (or alternatively ξ or μ) and M_c, the molecular weight between crosslinks from $2C_1$ using the Phantom approach. In addition, the small strain modulus, given by $2C_1 + 2C_2$ will be treated according to Graessley to estimate the entanglement trapping factor T_e, originally introduced by Langley [33] and which, according to Graessley [2] is related to the plateau modulus of the uncrosslinked material G_N:

$$G_{exp} = G_{chem} + G_N \cdot T_e . \tag{7}$$

Based on work on Ronca and Allegra [34], Flory and Erman [12, 13] and, independently, Kästner [35] developed theories which describe the real stress strain behavior as a perturbation of the phantom behavior only by local topological constraints (junction constraint theory, JCT). Phantom behavior is only approached in the limit of large extensions. Other theoretical models based on reptation theory have been developed taking account the topological incrossability of polymer chains, but these involve in general more complex mathematical treatments than the junction constraint approach and will not be used for data analysis in this paper. The basic concept of JCT is that fluctuations of the junctions are reduced through the presence of spatially neighbored junctions. According to Flory and Erman, trapped entanglements which are quoted to make a considerable contribution to network elasticity [2, 26] do not contribute to the network density by increasing the effective number of network chains but only by restricting junction fluctuations. As mentioned above, Graessley's treatment involves both reduction of junction fluctuations as well as long range topological restrictions due to trapped entanglements.

The Flory–Erman theory (JCT) describes the force as

$$[f^*] = [f_{ph}^*] \cdot [1 + f_c/f_{ph}] , \tag{8}$$

where $[f_{ph}^*]$ is the reduced force according to the phantom theory and f_c is the additional contribution of the constraints. The ratio f_c/f_{ph} is given by

$$f_c = \mu kT/L_0(V/V_0)^{1/3} \cdot [\alpha K(\lambda_1^2) - \alpha^{-2} K(\lambda_2^2)] , \tag{9}$$

where $K(\lambda_2)$ is a function of the deformation ratio with respect to the reference state (λ), K depends in complex manner on λ and two parameters (κ and ζ) in the following manner [12, 13, 31]:

$$K(\lambda^2) = B \cdot [\dot{B} \cdot (B + 1)^{-1} + g \cdot (\dot{g}B + g\dot{B}) \cdot (gB + 1)^{-1}] \tag{10}$$

$$B = (\lambda - 1)(1 + \lambda - f\lambda^2)/(1 + g)^2 \tag{11}$$

$$g = \lambda^2[\kappa^{-1} + \zeta(\lambda - 1)] \tag{12}$$

$$\dot{B} \equiv \frac{\partial B}{\partial \lambda^2} \tag{13}$$

$$\dot{g} \equiv \frac{\partial g}{\partial \lambda^2} = \kappa^{-1} - \varsigma(1 - 3\lambda/2) \tag{14}$$

$$\lambda_1 = \alpha(V/V_0)^{1/3} \tag{15}$$

$$\lambda_2 = \lambda_3 = \alpha^{-1/2}(V/V_0)^{1/3} . \tag{16}$$

κ describes the hindrance of fluctuations with respect to the phantom limit. In the limit of $\kappa \to \infty$ the JCT reduces to the affine limit, while for $\kappa \to 0$ the phantom limit is reached. ζ describes the change of the domains of constraints upon deformation. In another work Erman and Monnerie [36] give a new formulation where the constraints are not acting via the junctions, but via the center of mass of the surrounding chains.

However, the present analysis will be restricted to the "classical" Flory–Erman approach. An additional correction was made to account for the finite molecular mass of the starting materials. This turns out to be of importance for the lower molecular weight starting material (series PB_d-A-XX). To account for the effect of dangling chain ends in statistically crosslinked systems, Queslel and Mark [37] derived the following equations relating μ, ν, and ξ to the molecular weight between crosslinks and the molecular weight of the starting material for a tetrafunctional crosslinker:

$$\mu_a/V_0 = (\rho/2M_c)(1 - 2M_c/M_n) \quad (17)$$

$$\xi/V_0 = (\rho/2M_c)(1 - 3M_c/M_n) \quad (18)$$

$$\xi/V_0 = (\mu_a/V_0) - (\rho/M_n) \quad (19)$$

The effect of finite molecular weight and/or permanent entanglements on the cycle rank as it would be determined from elasticity measurements is shown schematically as a function of crosslinker concentration in Fig. 6. The straight line through the origin corresponds to the situation of a network without dangling chains, i.e., with primary chains of infinite length and no trapped entanglements. The lower curve would correspond to a network without entanglements, but containing dangling chains due to finite molecular weight of the starting material. This effect should be mostly compensated by the correction of Queslel and Mark. The upper curve, i.e., with an experimental cycle rank larger than the expected value from chemistry would correspond to networks where trapped entanglements play an important role in defining the elastic properties of the network.

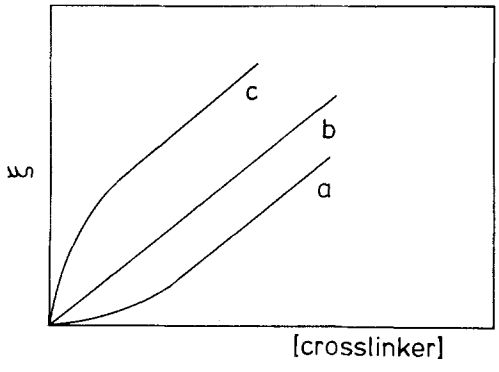

Fig. 6 Schematic representation of the dependence of the experimentally determined cycle rank from elasticity measurements for "ideal networks" (a), networks prepared from finite primary chains (b), networks with entanglement contribution to elasticity (c)

To analyze the mechanical data according to JCT, a nonlinear least square fit-program based on the Marquardt algorithm was developed. The input parameters for the calculation are the primary molecular weight, polymer concentration at which the network was formed, the degree of swelling at which the stress strain measurement was made and the stress strain curve from the Instron machine. From this curve fitting we obtain the cycle rank ξ, the number density of elastically effective junctions ν, the average molecular weight between junctions M_c, the junction constraint parameter κ, and the anisotropy parameter ζ. The program also allows to fix some or all of these parameters.

Analysis of the swollen networks

In this part the experimental results obtained from swollen networks (series PB_d-B-xx) will be discussed. In all cases the stress-strain curves can be described by the Mooney–Rivlin equation, i.e., a linear plot of the reduced force versus $1/\alpha$. In Table 5 the Mooney Rivlin constants $2C_1$ and $2C_2$ are listed together with the chemical crosslink density, expressed as molecular weight between junctions M_c^{chem} assuming complete reaction and the corresponding network molecular weights M_c^E and M_c^{Ph} obtained from small strain modulus $(2C_1 + 2C_2)$ and "phantom" limit $(2C_1)$, respectively. It is quite astonishing that both the analysis of the small strain modulus according to Eq. (1) and the analysis according to the Phantom theory $(2C_1)$ give values for M_c, which are considerably smaller than those predicted from stoichiometry. It might be argued that nonequilibrium states are responsible for these low

Table 5 Analysis of the stress-strain behavior of network series B, Mooney–Rivlin parameters and chain molecular weights calculated from stoichiometry, corrected for finite initial chain length and Eqs. (1) and (6)

Sample	$2C_1$ (N/mm²)	$2C_2$ (N/mm²)	M_c^{chem} (g/mol)	M_c^E Eq. (1) (g/mol)	M_c^{Ph} Eq. (6) (g/mol)
PB_d-B-025	0.312	0.496	24500	2850	3750
PB_d-B-030	0.333	0.439	20000	2990	3470
PB_d-B-060	0.508	0.492	9500	2300	2310

Colloid & Polymer Science, Vol. 273, No. 6 (1995)

M_c values. In Fig. 7 the $2C_1$ constant multiplied by $v_2^{-1/3}$ is plotted as a function of the volume fraction v_2, to account for the change in chain concentration upon swelling. As expected theoretically, parallel lines are observed for three different crosslink densities. If time-dependent phenomena would interfere, a different behavior would be expected for the swollen networks, where relaxation is expected to occur much faster. Thus, the low M_c values, as an indication of a large number of elastically effective network chains, show that permanent, trapped entanglements additionally contribute to the modulus in polybutadiene networks. In the case of the high molecular weight starting material their contribution even dominates the behavior.

In most of the published work where JCT theory was used to describe the elastic behavior of elastomer networks, model networks prepared by endlinking chemistry have been used. In these systems the cycle rank ξ either was taken directly from the stoichiometry assuming complete reaction or corrected after performing an extended sol-gel analysis. Statistically crosslinked networks of polyisoprene were obtained by peroxide curing [38]. In that case the cycle rank ξ was determined by a fit of the experimental data using F.E.T. An analysis of the mechanical behavior of statistically crosslinked polybutadiene using a multifunctional silane crosslinker was presented by Brotzmann et al. [39]. There the cycle rank was obtained from the chemistry after sol-gel analysis. It is implicitly assumed that trapped entanglements do not act as permanent crosslink junctions.

In the following analysis of experimental data using JCT, we will try to check how reliably the cycle rank, as the most important molecular parameter which characterizes the network structure, can be determined by the curve fitting procedure. This is not a simple task, because experimental data only are available in a limited range of rather small strains, while an unambiguous determination of ξ requires knowledge of the stess-strain behavior up to large strains due to the nonlinearity of the theoretical curves in the usual Mooney–Rivlin representation.

Though a defined chemical reaction was used to introduce the chemical crosslinks, ξ was not calculated from the number of chemical junctions, because trapped entanglements might give an additional contribution to the cycle rank in the case of polybutadiene which is known to have a high plateau modulus in the melt [2]. In addition, the classical analysis already indicated that chemical crosslinking alone is not sufficient to explain in $2C_1$ values.

It is expected that for networks swollen to different v_2, the parameters ξ, ν and μ, but also κ and ζ are identical. Thus, the nonlinear least square fit applied to the stress strain data of a network swollen to different degrees can be used to check the internal consistency of the experimental data.

In Fig. 8 the reduced force $[f^*]$ is plotted as a function of the reciprocal macroscopic strain ratio α^{-1} for PB_d-B-60 swollen to different degrees. The force already has been reduced according to Eq. (3) for swelling. The curves represent the best fit using JCT to the experimental data by varying ν, κ and ζ. Corresponding fit parameters are listed in Table 6. Though the available strain range is rather limited, especially for the networks with a low degree of swelling, the calculated ordinate values of the reduced force axes obtained from the "free" fit are in astonishing good coincidence. They only vary in a range of 0.51 ± 0.03. The values of κ and ζ show only very small variation. In Fig. 9 the theoretical curves were recalculated using $\xi = 2.26\ 10^{-4}$ mol/cm^3, $\kappa = 15$, $\zeta = 0.1$. These are about the average values obtained from the fits given in Fig. 8. Comparison of the calculated curves with the experimental data shows rather good agreement. Only a very small decrease in $[f^*_{ph}]$ and thus μ is observed with increasing degree of swelling in the experimental data as well as

Fig. 7 Analysis of swollen networks according to the Mooney–Rivlin equation; plot of $2C_1 \cdot v_2$-1/3 versus v_2 for network series B; PB_d-060 (■); PB_d-030 (▲); PB_d-025 (●)

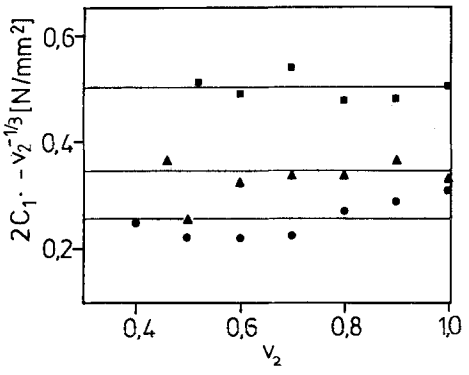

Fig. 8 Fit of the Flory–Erman theory (full curve) to the reduced force $[f^*]$ of network PB_d-B-060 swollen to different degrees in polybutadiene oligomer (best fit results, for fit parameters see Table 6) $v_2 = 1.0$(○) ; 0.9 (△); 0.8 (⬡); 0.7 (□); 0.6 (●); 0.5 (▲)

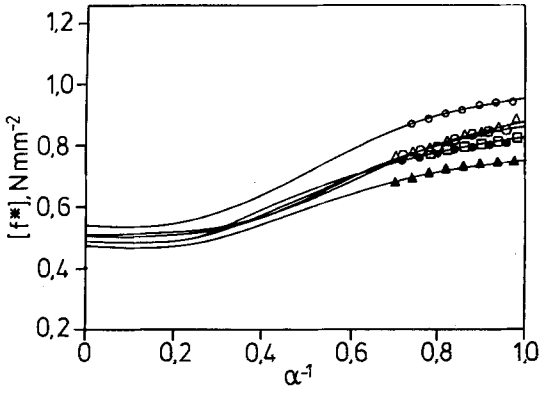

Table 6 Fit parameters resulting from nonlinear fit of swollen PB_d-B-xx networks to the Flory Erman theory

v_2	$\mu \cdot 10^4$ (mol/cm^3)	$\xi \cdot 10^4$ (mol/cm^3)	κ	ζ	$[f^*_{ph}]$ (N/mm^2)
PB_d-B-060					
1.0	2.14	2.08	18.0	0.038	0.546
0.9	2.09	2.07	21.2	0.094	0.519
0.8	2.07	2.04	23.6	0.062	0.512
0.7	1.97	1.95	21.7	0.0265	0.495
0.6	2.00	1.98	22.8	0.024	0.500
0.5	1.93	1.90	22.3	0.025	0.480
PB_d-B-030					
1.0	1.82	1.79	15.0	0.104	0.446
0.9	1.83	1.83	17.4	0.098	0.455
0.8	1.75	1.73	8.0	0.125	0.435
0.7	1.74	1.71	12.8	0.078	0.431
0.6	1.58	1.56	9.6	0.107	0.392
0.5	1.45	1.42	16.2	0.124	0.359
PB_d-B-025					
1.0	1.58	1.55	24.5	0.106	0.398
0.9	1.54	1.51	22.4	0.070	0.383
0.8	1.30	1.27	13.8	0.082	0.322
0.7	1.27	1.24	14.3	0.101	0.316
0.6	1.21	1.18	16.6	0.113	0.300
0.5	1.21	1.19	14.3	0.094	0.303
0.4	1.21	1.18	19.2	0.058	0.301

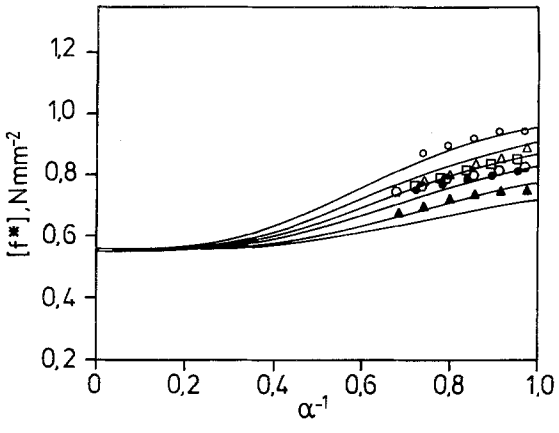

Fig. 9 Fit of the Flory–Erman theory (full curve) to the reduced force $[f^*]$ of network PB_d-B-060 swollen to different degrees in polybutadiene oligomer (average fit parameters, see text), symbols as in Fig. 8

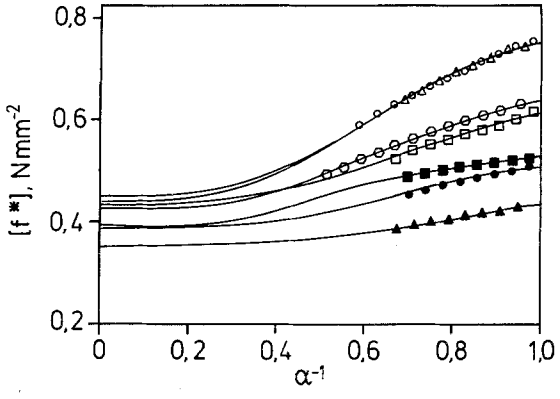

Fig. 10 Fit of the Flory–Erman theory (full curve) to the reduced force $[f^*]$ of network PB_d-B-030 swollen to different degrees in polybutadiene oligomer (best fit results, for fit parameters see Table 6) v_2 = 1.0 (○); 0.9 (△); 0.8 (◯); 0.7 (□); 0.6 (■); 0.5 (●); 0.4 (▲)

the theoretical fit. A similar good agreement between theoretical curves and experimental data has been obtained for networks with two other crosslink densities at different degrees of swelling. In Figs. 10 and 11 the experimental reduced force data $[f^*]$ are shown together with the theoretical curves. The corresponding "best fit" parameters are also listed in Table 6.

From this analysis we conclude that a reasonable and consistent description of the stress strain properties in uniaxial extension can be made by the JCT. However as already anticipated before, the chemical junction density is not sufficient to explain the crosslink density. Thus, permanent entanglements have to be taken into account.

Networks with varying crosslink density

In this part, the mechanical properties of a series of networks with a widely varying degree of crosslink density is

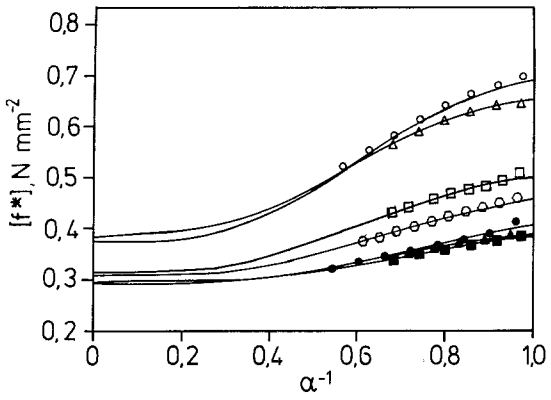

Fig. 11 Fit of the Flory–Erman theory (full curve) to the reduced force $[f^*]$ of network PB_d-B-025 swollen to different degrees in polybutadiene oligomer (best fit results, for fit parameters see Table 6) v_2 = 1.0(○); 0.9 (△); 0.8 (□); 0.7 (◯); 0.6 (●); 0.5 (■); 0.4 (▲)

analyzed using classical theories, JCT and the trapped entanglement approach by Graessley. Based on the analysis of networks with different degrees of swelling, we feel quite confident that a fit of Eq. (8) to the experimental data gives a reasonable estimate of an efficient cycle rank ξ and also of κ. The anisotropy parameter ζ generally remains rather small and might be subject to considerable variation, probably due to experimental error. No attempts to discuss ζ will be made.

The networks have been prepared using a deuterated polybutadiene of molecular weight 80 000 g/mol, which is much smaller than the polybutadiene used for the networks in the previous section. Thus, the influence of dangling ends is of considerable importance in the case of small crosslink densities and the correction for this finite primary molecular weights according to Queslel and Mark (Eqs. (17–19)) has been taken into account. The concentration of crosslinker 4 has been varied between 0.1 and 1.5 mol%, corresponding to a theoretical range of molecular weights between crosslink junctions between 54 000 g/mol and 3600 g/mol if dangling chain ends are not considered. Experimental results of the stress strain behavior, obtained from the Mooney–Rivlin equation and the M_c values calculated from stoichiometry (taking account for the finite molecular weight of PB_d-A) and according to Eqs. [1] and [6] are given in Table 7.

In Fig. 12 the reduced force $[f^*]$ is plotted as a function of $1/\alpha$. The experimental data are fitted to the junction constraint theory allowing variation of ξ, κ, and ζ. The curves correspond to the best fit. The corresponding fit parameters are listed in Table 8. As in the previous section the FE-theory allows a reasonable description of the experimental data.

In Fig. 13 the cycle rank ξ is plotted as a function of the network chain density ρ/M_c^{chem} calculated from the amount of crosslinker. For higher crosslinker concentrations a straight line is observed which clearly shows a finite positive ordinate. For the lowest crosslinker concentrations a deviation from this linear behavior is observed. As has been discussed earlier, only a positive ordinate is expected if trapped entanglements increase the number of elastically effective chains ($\sim\xi$). Included in Fig. 13 are the corresponding values obtained from crosslinking of the longer primary chains (series B). In this case the estimated ordinate is much larger, indicating that the number of trapped elastically effective entanglements is considerably larger in the case of the longer primary chains.

In Fig. 14 the junction constraint parameter κ is shown as a function of network chain density concentration. For the polybutadiene networks we observe constant value of κ in the order of 20. Only at the very low degrees of crosslinking does κ strongly increases.

Based on the small strain modulus $(2C_1 + 2C_2)$ the trapping factor T_e was calculated according to Eq. (7). The data are represented in a "Langley"-plot by plotting G_{exp}/T_e against G_{chem}/T_e (Fig. 15). The theoretical modulus G_{chem} was obtained by taking account for the finite primary molecular weight assuming random crosslinking. The corresponding data are collected in Table 9 for series A and B. The trapping parameter of series A (low primary molecular weight) increases from about 0.1 to 0.4 with increasing crosslink density. For series B the trapping factor is in the order of 0.6, close to the value of Dossin and Graessley for networks of comparable crosslink density.

Table 7 Analysis of the stress-strain behavior of network series A, Mooney–Rivlin parameters and chain molecular weights M_c calculated from stoichiometry corrected for finite molecular weight and Eqs. (1) and (6)

Sample	$2C_1$ (N/mm²)	$2C_2$ (N/mm²)	M_c^{chem} (g/mol)	M_c^E Eq (1) (g/mol)	M_c^{ph} Eq (6) (g/mol)
PB_d-A-010	0.0180	0.033	–	45 180	63 300
PB_d-A-015	0.0475	0.115	360 000	14 180	22 450
PB_d-A-020	0.0584	0.099	83 000	14 640	19 600
PB_d-A-035	0.1190	0.320	40 000	5 250	9 700
PB_d-A-050	0.236	0.336	14 790	4 030	4 720
PB_d-A-075	0.261	0.398	8 780	3 500	4 350
PB_d-A-100	0.412	0.443	6 240	2 700	2 780
PB_d-A-150	0.564	0.490	3 950	2 190	2 035

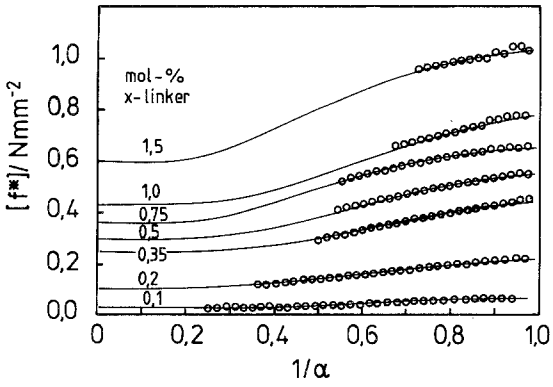

Fig. 12 Reduced force $[f^*]$ as a function of reciprocal strain ratio y^{-1} for network series A, curves represent best fit according to JCT

Aranguren and Macosko published an analysis on small strain moduli of polybutadienes prepared by hydrosilylation reaction [26]. They used lower molecular weight starting materials and prepared networks of much higher chemical crosslink density. For those samples where the modulus is comparable to our systems, trapping factors are of the same order. The plateau modules G_N of polybutadiene was taken from ref. [2]. The trapping factors are smaller than those reported by Dossin and Graessley, probably due to the fact that in the limit of very low crosslink density only few entanglements are permanently trapped. A more detailed interpretation of the trapping factor is given in ref. [2].

The analysis for the present network shows for network series A that the small strain modulus is about twice the value of the theoretical value as obtained from stoichiometry. If the modulus is split into contributions to $2C_1$ and $2C_2$, it turns out that trapped entanglements significantly contribute to $2C_1$. This is seen also from Fig. 16, where $2C_1$ is plotted as a function of the network chain density, as calculated from stoichiometry. While in the absence of trapped entanglements extrapolation to $\rho/M_c^{chem} = 0$ would yield $2C_1 = 0$, a positive intercept is found, which is due to trapped entanglements. The linear dependence of $2C_1$ from ρ/M_c^{chem} shows further that the amount of trapped entanglements is independent of the chemical crosslink density for high primary molecular weight materials (series B). For series A, on the other hand, at low crosslink densities the amount of trapped entanglements varies with crosslink density, indicating the influence of dangling chain ends on the trapping factor.

Networks crosslinked in concentrated solution

The last series of networks (PB_d-L-xx) to be discussed has been prepared at constant crosslink density at varying polymer concentration. The stress strain curves of the dry networks are shown in Fig. 17.

With decreasing polymer concentration the stress at a given strain is lower and larger ultimate strains are reached. The corresponding Mooney–Rivlin plots are linear. The Mooney–Rivlin constants are listed in Table 10. According to the discussion concerning the choice of the reference state, the modulus has to be multiplied by $v_{2c}^{-2/3}$ to account for the solution crosslinking. The corresponding data are also collected in Table 10. The values obtained for the high polymer concentrations are about the same within experimental errors, while higher values for $(2C_1 + 2C_2)$ and $2C_1$ are obtained for $v_{2c} = 0.08$ and 0.15. The deviation is larger for the reduced small strain modulus. Two effects might be responsible for the different behavior of these samples. First, it is much more difficult to reach mechanical equilibrium in networks crosslinked in dilute solution, probably due to the different network topology which allows network unfolding [11, 40] and the increased modulus values might be attributed to nonequilibrium states. This effect might give a significant contribution to the small strain modulus while the influence on $2C_1$ should be rather small. The second, more significant effect arises from the observation that partial deswelling was observed during network preparation, i.e., a part of the solvent was expelled during the crosslink reaction. As a consequence the volume fraction v_{2c} varied during the curing process and was larger than in the original solution. Thus, the correction term $v_{2c}^{-2/3}$ becomes

Table 8 Curve fitting parameters for network series A according to junction constraint theory

Sample	$\mu \cdot 10^4$ (mol/cm³)	$\xi \cdot 10^4$ (mol/cm³)	κ	ζ	$[f_{ph}^*]$ (N/mm²)
PB_d-A-010	0.227	0.111	50.0	0.11	0.056
PB_d-A-015	0.571	0.455	40.0	0.145	0.141
PB_d-A-020	0.565	0.448	34.4	0.116	0.139
PB_d-A-035	1.110	0.990	30.0	0.135	0.273
PB_d-A-050	1.334	1.212	21.4	0.082	0.330
PB_d-A-075	1.584	1.467	19.3	0.050	0.391
PB_d-A-100	0.874	1.758	20.5	0.095	0.462
PB_d-A-150	2.559	2.443	12.85	0.053	0.629

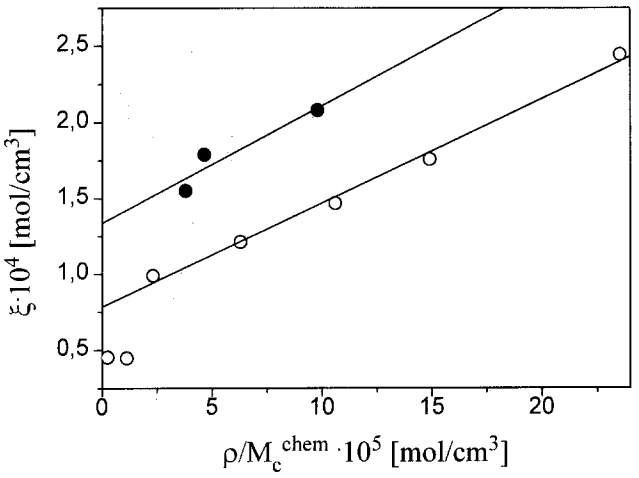

Fig. 13 Cycle rank ξ, obtained from the fit of JCT to network series A (○) and B (●) as a function of chemical network chain density ρ/M_c^{chem}

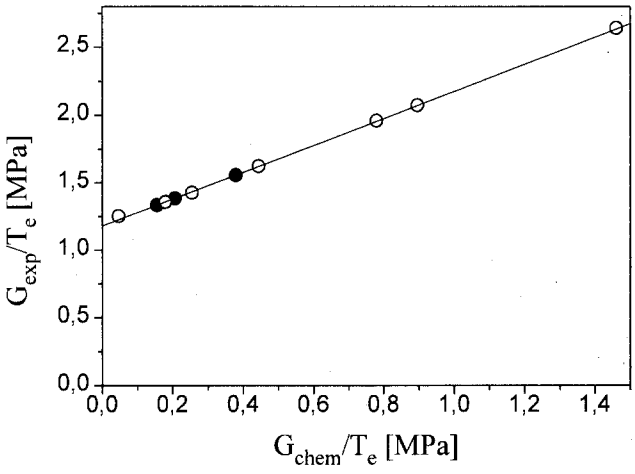

Fig. 15 "Langley"-plot G_{exp}/T_e versus G_{chem}/T_e for network series A (○) and B (●) (data taken from Table 9)

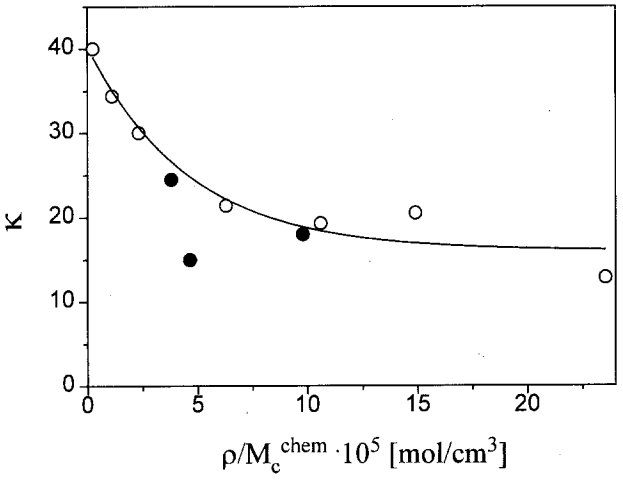

Fig. 14 Junction constraint parameter κ obtained from fitting JCT to experimental stress strain data as a function of chemical network chain density ρ/M_c^{chem}; network series A (○), B (●)

too large. Of course these networks are rather illdefined, because of these concentration changes during the reaction. Any attempt to fit these stress strain curves with JCT failed, the $2C_2$ parameter is much larger than $2C_1$. Such stress strain curves cannot be described by the junction constraint theory. The same problem already occurs for network PB_d-L-025. The fit of JCT to the remaining experimental data for the networks prepared at higher concentrations is shown in Fig. 18. The corresponding fit parameters are listed in Table 10. Only for $v_{2c} = 1$, 0.75 and 0.5 is a good fit obtained, resulting in a constant cycle rank ξ, while the fit fails for $v_{2c} = 0.25$ and below. Extreme values for κ and μ result from the fit. However, only for $v_{2c} = 1$ and $v_{2c} = 0.75$ the parameter κ is proportional to $2C_1^{-0.5} \cdot v_{2c}^{4/3}$, as predicted by the JCT. This again reflects that crosslinking in rather dilute systems leads to irregular network topologies, which are beyond the framework of the classical JCT. No attempts have been made to apply

Table 9 Experimental small strain shear modulus ($2C_1 + 2C_2$), theoretical shear modulus G_{chem}, trapping factor T_e and T_eG_N for network series A and B

Sample	$2C_1 + 2C_2$ (MPa)	G_{chem} (corrected) (MPa)	T_e	T_eG_N (MPa)
PB_d-A-010	0.051	–	–	–
PB_d-A-015	0.163	0.006	0.13	0.156
PB_d-A-020	0.157	0.028	0.11	0.123
PB_d-A-035	0.439	0.058	0.323	0.381
PB_d-A-050	0.572	0.156	0.352	0.415
PB_d-A-075	0.659	0.262	0.336	0.4
PB_d-A-100	0.855	0.369	0.412	0.49
PB_d-A-150	1.054	0.583	0.399	0.471
PB_d-B-025	0.808	0.094	0.605	0.72
PB_d-B-030	0.772	0.115	0.557	0.66
PB_d-B-060	1.000	0.243	0.642	0.76

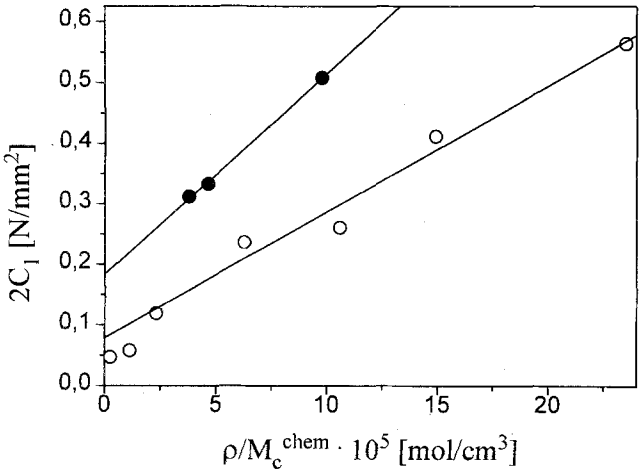

Fig. 16 Mooney-Rivlin parameter $2C_1$ as a function of the chemical network chain density ρ/M_c^{chem}; network series A (○), B (●)

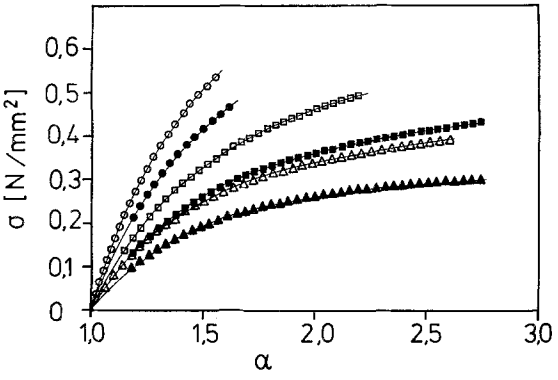

Fig. 17 Stress strain curves for network series PB_d-L-xx; (▲) PB_d-L-008; (△) PB_d-L-015; (■) PB_d-L-025; (□) PB_d-L-050; (●) PB_d-L-075; (○) PB_d-L-100

Table 10 Mechanical characterization of solution crosslinked polybutadiene networks

Probe	$2C_1$	$2C_2$	$2C_1 \cdot v_{2c}^{-2/3}$	$(2C_1 + 2C_2) \cdot v_c^{-2/3}$
	(N/mm^2)	(N/mm^2)	(N/mm^2)	(N/mm^2)
PB_d-L-008	0.054	0.225	0.290	1.5
PB_d-L-015	0.086	0.252	0.305	1.2
PB_d-L-025	0.125	0.240	0.264	0.92
PB_d-L-050	0.143	0.272	0.226	0.66
PB_d-L-075	0.212	0.305	0.257	0.63
PB_d-L-100	0.271	0.378	0.271	0.65

the modified formulation given by Monnerie and Erman [36], which should allow the representation of stress strain curves where $2C_2 > 2C_1$.

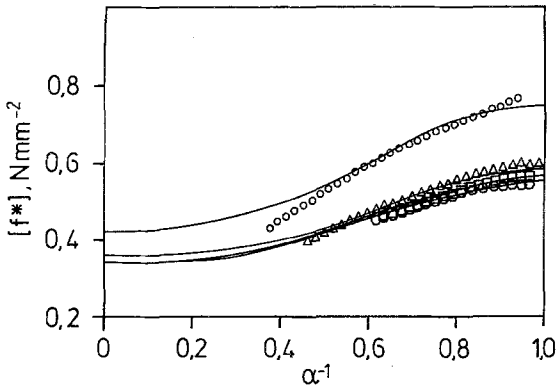

Fig. 18 Reduced force $[f^*]$ as a function of reciprocal strain ratio α^{-1} for network series PB_d-L-xx, curves represent best fit according to JCT. (○) PB_d-L-025; (△) PB_d-L-050; (◯) PB_d-L-075; (□) PB_d-L-100

Table 11 Fit-parameter according to the Flory–Erman theory of solution crosslinked networks

v_{2c}	$\mu \cdot 10^4$	$\xi \cdot 10^4$	κ	ζ	$[f_{ph}^*]$
	(mol/cm^3)	(mol/cm^3)			(N/mm^2)
1.00	1.42	1.39	13.9	0.12	0.350
0.75	1.42	1.39	12.4	0.10	0.351
0.50	1.48	1.45	26.0	0.35	0.366
0.25	1.72	1.70	37.3	1.15	0.426
0.15[a)]	–	–	–	–	–
0.08[a)]	–	–	–	–	–

[a)] no fit according to JCT possible, details see text

Conclusions

It has been shown in the previous discussion that defined polybutadiene networks of varying crosslink density can be prepared by the reaction of linear high molecular weight polybutadiene with a masked bistriazolinedione. This method provides the possibility of network preparation in bulk and in solutions of varying concentration. Analysis of the stress strain behavior according to affine, "Phantom" and junction constraint theory (JCT) gives clear evidence that permanent trapped entanglements contribute considerably to the elastically effective number of network chains. This is supported by the analysis of the small strain modulus data according to Graessley [2]. Interestingly, the effect of permanent trapped entanglements is more pronounced, if high molecular weight starting material is used, though the effect of finite chain length has been taken into account. Further experiments, involving a broader range of primary molecular weights will be necessary to elucidate this observation in more detail. The junction constraint theory is found to give a reasonable description of the experimental data in most cases, if one

allows contributions of both chemical crosslinks and trapped entanglements to the cycle rank, though trapped entanglements are beyond the underlying theoretical concept. Description of data was found to fail with this theory, when the crosslinking process was performed in dilute solutions, since this probably leads to very heterogeneous network topologies.

The networks characterized in the present study were made from partially deuterated polybutadienes. The main objective of this work is the investigation of the segmental orientation behavior of deuterated networks and deuterated probe molecules in the same network. Details of ^{2}H-NMR- and strain birefringence studies will be published in a forthcoming paper [41].

Acknowledgement This work has been supported by Stiftung Volkswagen-Werk through the joint project Freiburg (Germany)–Porto Alegre (Brazil) and Deutsche Kautschuk-Gesellschaft (project 7/93). M.M.J. and L.L.F. received fellowships from Deutscher Akademischer Austauschdienst (DAAD) which is gratefully acknowledged. The Bruker-IFS 88 FT-IR-spectrometer was available through the joint project BASF/Freiburg supported by the Bundesministerium für Forschung und Technologie. The authors are indebted to S. Auerbach, Dr. J. Rösch, and Dr. G. Person for technical assistance. R.S. is indebted to Prof. W.W. Graessley (Princeton) for his valuable comments concerning to the analysis of the small strain moduli.

References

1. Gottlieb M, Macosko CW, Benjamin GS, Meyers KO, Merrill EW (1981) Macromolecules 14:1039
2. Dossin L, Graessley WW (1989) Macromolecules 12:123
3. Mark JE, Erman B (eds) Rubber Elasticity – A Molecular Primer I Ed, John Wiley & Sons, New York 1988
4. Rout SP, Butler GB (1980) Polymer Bulletin 2:513
5. Stadler R, Jacobi MM, Gronski W (1983) Makromol Chem Rapid Commun 4:129
6. Freitas L, Jacobi MM, Stadler R (1984) Polymer Bulletin 11:408
7. Butler GB (1980) Ind Eng Chem Prod Res Dev 19:512
8. Stadler R, Freitas L, Jacobi MM (1986) Makromol Chem 188:823
9. Stadler R, Bühler F, Gronski W (1986) Makromol Chem 188:1301
10. de Lucca Freitas L (1985) Tese de Mestrado, Porto Alegre
11. Gronski W, Stadler R, Jacobi MM (1984) Macromolecules 18:841
12. Flory PJ, Erman B (1982) Macromolecules 15:800
13. Erman B, Flory PJ (1982) Macromolecules 15:806
14. Erman B, Flory PJ (1983) Macromoleeules 16:1608
15. Stadler R, Abetz V, Jacobi MM (1985) Polymer Bulletin 14:318
16. Seymour CA, Greene FD (1980) J Am Chem Soc 102:6384; Cheng CC, Seymour CA, Petti MA, Greene FD (1984) J Org Chem 49:2910
17. Jacobi MM, Stadler R (1988) Makromol Chem Rapid Commun 9:709
18. Fleming MP, McMurry JE (1981) Org Synthesis 60:113
19. Jacobi MM, Dissertation, University of Freiburg 1989
20. Jacobi MM, Stadler R, Stibal E, Gronski W (1986) Makromol Chem Rapid Commun 8:443
21. Chambon F, Petrovic ZS, MacKnight WJ, Winter HH (1986) Macromolecules 19:2146
22. Chambon F, Winter HH (1987) J Rheol 31:683
23. Hess W, Vilgis TA, Winter HH (1988) Macromolecules 21:2536
24. Rubinstein M, Colby RH, Gillmor JR (1989) Polym Prepr Am Chem Soc 30(1):81
25. Martin JE, Adolf D, Wilcoxon JP (1989) Polym Prepr Am Chem Soc 30(1):83
26. Aranguren MI, Macosko CW (1988) Macromolecules 21:2484
27. Winter HH private communication
28. Kuhn W (1936) Colloid Polym Sci 68:2
29. Treloar LRG (ed) Principles of Rubber Chemistry. 3rd Ed, Clarendon Press, Oxford 1985
30. James HM, Guth E (1949) J Polym Sci 4:153
31. Flory PJ (1986) Proc R Soc Lond A351:351
32. Queslel JP, Mark JE (1985) Adv Polym Sci 65:135
33. Langley NR (1968) Macromolecules 1:348
34. Ronca G, Allegra G (1988) J Chem Phys 68:5363
35. Kästner S (1980) Acta Polymerica 31:444
36. Erman B, Monnerie L (1989) Macromolecules 22:3342
37. Queslel JP, Mark JE (1985) J Chem Phys 82:3449
38. Queslel JP, Thirion P, Monnerie L (1986) Polymer 27:1869
39. Brotzmann RW, Flory PJ (1987) Macromolecules 20:351
40. Ullmann R (1982) Macromolecules 15:582
41. Jacobi MM, Stadler R, Abetz V, Gronski W (in preparation)